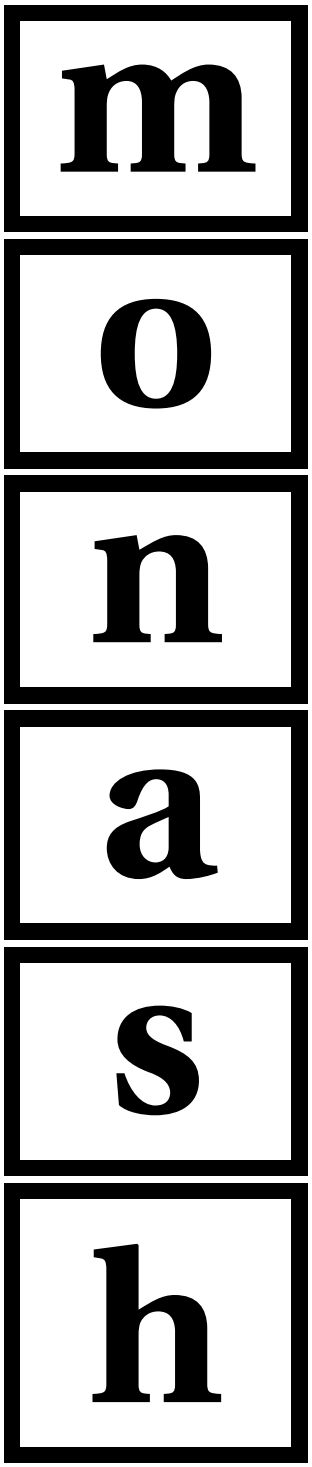

MECSE 1992-1

Fast Evaluation of Radial Basis/Spline Functions: Multipoles Without Multipoles

D. Suter

21 October 1992

TECHNICAL REPORT
DEPARTMENT OF ELECTRICAL AND
COMPUTER SYSTEMS ENGINEERING,
FACULTY OF ENGINEERING,
MONASH UNIVERSITY, CLAYTON 3168,
VIC, AUSTRALIA

Fast Evaluation of Radial Basis/Spline Functions: Multipoles Without Multipoles

D. Suter
Dept. of Electrical and Computer Systems Engineering
Monash University
Clayton, 3168
Australia

21 October 1992

1 Introduction

The multipole expansion [CGR88] is a computational technique that can be utilized in the calculation of the potential produced by individual sources. It has immediate application in the large scale simulation of interacting particles.

Recently, Beatson and Newsam [BN92] have suggested using such techniques for the rapid evaluation of thin-plate splines. The thin-plate spline is a method of data approximation that is analogous to attaching a thin flexible metal plate to the data points with springs between the data points and the plate. Mathematically, it can be shown [Wah90] that the solution can be expressed in terms of the linear combination of spline kernels $r^2 \log r$ centered at each data point. The essential idea is that the thin-plate spline formulation reduces to a matrix equation that needs to be solved for the linear coefficients of these kernels and, subsequently, the matrix equations need to be evaluated to produce values for the function approximating the data at other points. Being able to rapidly evaluate the linear combination of these kernel functions would be an advantage in both the solution stage (allowing iterative solution methods) as well as the evaluation stage.

Thin-plate splines arise in the context of computer vision through a regularization formulation [BZ87]. Thus we expect the techniques discussed here to have applications in many of the areas of low level vision (see, for example, [Ter82] [BZ87]).

The contribution of this paper is to take the suggestion of Beatson and Newsam [BN92], which uses the standard multipole expansions [CGR88], and to develop an alternative approach motivated by the work of Anderson [And92]. This approach replaces the multipole expansion with the evaluation of an expansion along a closed contour surrounding the centres of the potential functions.

1.1 Notation

In the following, we use the complex plane to represent R^2 and a point in the plane is denoted by $z = re^{i\theta}$ We will sometimes express a given function in two ways: e.g., $E(z)$ or $E(r, \theta)$ depending upon whether it is more convenient to use the polar form. The complex conjugate of z is denoted $\overline{z}$. The real and imaginary parts of z are denoted $\mathcal{R}\{z\}$ and $\mathcal{I}\{z\}$.

2 Expansion for Thin-Plate Kernel

It is known (see [SNWC77] p. 147) that a real function which is biharmonic on the punctured plane (missing the origin) can be represented as:

$$\begin{aligned} u &= (a+br^2)\log r + r\log r\cdot(c\cos\theta + d\sin\theta) \\ &\quad + \sum_{n=-\infty}^{n=\infty} r^n(a_n\cos n\theta + b_n\sin n\theta) + r^{n+2}(c_n\cos n\theta + d_n\sin n\theta). \end{aligned} \tag{1}$$

In this section, we will see how to derive the coefficients or approximations to the coefficients of the general form. We use this to then derive two approximations: one valid far from the centre of expansion (which corresponds to the Laurent series expansion of [BN92] and the outer ring approximation of [And92]), and one valid near the centre of expansion (the Taylor series expansion or inner ring expansion).

Recently, Beatson and Newsam [BN92] have shown that a collection of m thin-plate kernels (each of which is biharmonic on the punctured plane) each centered at z_j,and with (real) coefficient d_j, has an expansion:

$$\begin{aligned} \Phi(z) &= \sum_{j=1}^{m} d_j|z-z_j|^2\log|z-z_j| \\ &= \left[\alpha|z|^2 - 2\mathcal{R}\left\{\overline{\beta}z\right\} + \gamma\right]\log|z| + \mathcal{R}\left\{\sum_{k=0}^{\infty}(a_k\overline{z}+b_k)z^{-k}\right\}. \end{aligned} \tag{2}$$

The values of the constants a_k and b_k do not concern us here, but we will need the following:

$$\alpha = \sum_{j=1}^{m} d_j, \tag{3a}$$

$$\beta = \sum_{j=1}^{m} d_j z_j, \tag{3b}$$

$$b_0 = \gamma = \sum_{j=1}^{m} d_j|z_j|^2. \tag{3c}$$

Our immediate aim is to find an alternative expression for the multipole expansion (the last term in 2). Define:

$$\begin{aligned} E(r,\theta) &= \Phi(r,\theta) - \left[\alpha|z|^2 - 2\mathcal{R}\left\{\overline{\beta}z\right\} + \gamma\right]\log|z| \\ &= \mathcal{R}\left\{\sum_{k=0}^{\infty}(a_k\overline{z}+b_k)z^{-k}\right\} \\ &= \mathcal{R}\left\{\sum_{k=1}^{\infty}(a_{k-1}r^2+b_k)r^{-k}e^{-ik\theta}\right\} + b_0. \end{aligned} \tag{4}$$

From the last expression we can see that, for fixed a and b, $a \neq b$, and for $k \geq 1$:

$$\int_0^{2\pi} E(a,s)e^{iks}\,ds = \pi(a_{k-1}a^2+b_k)a^{-k}, \tag{5a}$$

$$\int_0^{2\pi} E(b,s)e^{iks}\,ds = \pi(a_{k-1}b^2+b_k)b^{-k}. \tag{5b}$$

The key is that this gives us two equations in two unknowns, i.e., the coefficients a_k and b_k. We can use the first expression in equation 4 to numerically approximate the left hand sides in equations 5a and 5b. Before we do this, it is simple to solve for the coefficients:

$$a_{k-1} = \frac{1}{\pi}\frac{1}{a^2-b^2}\left(a^k\int_0^{2\pi}E(a,s)e^{iks}\,ds\; -b^k\int_0^{2\pi}E(b,s)e^{iks}\,ds\right), \tag{6a}$$

$$b_k = \frac{1}{\pi}\frac{1}{a^2-b^2}\left(-b^2a^k\int_0^{2\pi}E(a,s)e^{iks}\,ds\; +a^2b^k\int_0^{2\pi}E(b,s)e^{iks}\,ds\right). \tag{6b}$$

We substitute these into equation 4, interchange the summations and integrations, and truncate the summations at term $k = M$ (this truncation is to avoid the "aliasing" effects that Anderson reports with his log kernels [And92]):

$$\begin{aligned} E(r,\theta) &= \mathcal{R}\left\{\frac{1}{\pi}\frac{1}{a^2-b^2}\int_0^{2\pi}(r^2-b^2)E(a,s)\left(\sum_{k=1}^{M}(\frac{a}{r})^k e^{-ik(\theta-s)}\right)\right. \\ &\left.+(a^2-r^2)E(b,s)\left(\sum_{k=1}^{M}(\frac{b}{r})^k e^{-ik(\theta-s)}\right)\,ds\right\}+b_0. \end{aligned} \tag{7}$$

Finally, it is easy to sum the two geometric series and take the real parts (see appendix A) to obtain:

$$\begin{aligned} E(r,\theta) = \frac{1}{\pi}\frac{1}{a^2-b^2}\int_0^{2\pi} & \\ (r^2-b^2)E(a,s)\frac{-(\frac{a}{r})^{M+1}\cos((M+1)(\theta-s))+(\frac{a}{r})^{M+2}\cos(M(\theta-s))+\frac{a}{r}\cos(\theta-s)-(\frac{a}{r})^2}{1-2(\frac{a}{r})\cos(\theta-s)+(\frac{a}{r})^2}+ & \\ (a^2-r^2)E(b,s)\frac{-(\frac{b}{r})^{M+1}\cos((M+1)(\theta-s))+(\frac{b}{r})^{M+2}\cos(M(\theta-s))+\frac{b}{r}\cos(\theta-s)-(\frac{b}{r})^2}{1-2(\frac{b}{r})\cos(\theta-s)+(\frac{b}{r})^2}\,ds & \\ +b_0. & \end{aligned} \tag{8}$$

3 Evaluation of the Expansion

To calculate the value of the expansion involves, in principle, choosing two closed curves (circles of radii a and b for simplicity - see figure 1) and approximating the respective integrals in equation 8 by some numerical quadrature. We use the simple strategy of breaking the circle up into K equally spaced angular sections $h = \frac{2\pi}{K}$. To simplify the expressions we define:

$$\mathcal{K}(a,r,\theta,s,M) = \frac{-(\frac{a}{r})^{M+1}\cos((M+1)(\theta-s))+(\frac{a}{r})^{M+2}\cos(M(\theta-s))+\frac{a}{r}\cos(\theta-s)-(\frac{a}{r})^2}{1-2(\frac{a}{r})\cos(\theta-s)+(\frac{a}{r})^2}. \tag{9}$$

We can then approximate the terms in 8 by:

$$\begin{aligned} E(r,\theta) &= \frac{1}{\pi}\frac{1}{a^2-b^2}\sum_{i=1}^{K}\Big((r^2-b^2)E(a,s_i)\mathcal{K}(a,r,\theta,s_i,M)h+(a^2-r^2)E(b,s_i)\mathcal{K}(b,r,\theta,s_i,M)h\Big) \\ &\quad +\gamma. \end{aligned} \tag{10}$$

Similar reasoning (see appendix B) allows us to derive the inner ring approximation:

$$\Phi(r,\theta) = \frac{1}{\pi}\frac{1}{a^2-b^2}\sum_{i=1}^{K}\Big((r^2-b^2)\Phi(a,s_i)\mathcal{K}'(a,r,\theta,s_i,M)h+(a^2-r^2)\Phi(b,s_i)\mathcal{K}'(b,r,\theta,s_i,M)h\Big), \tag{11}$$

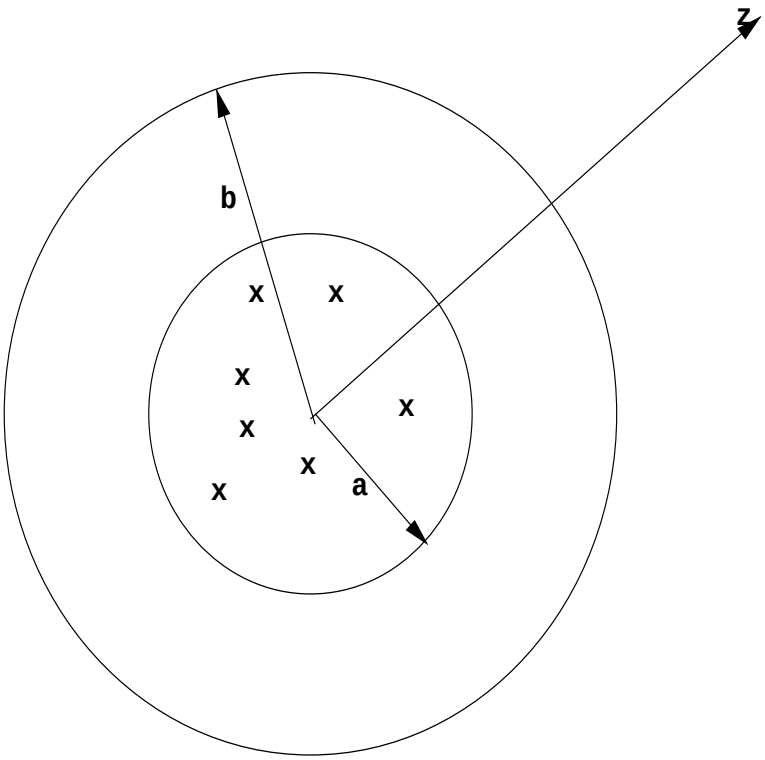

Figure 1: Outer Ring Expansion

where we have defined:

$$\mathcal{K}'(r,a,\theta,s,M) = \frac{(\frac{r}{a})^{M+2}\cos(M(\theta-s)) - (\frac{r}{a})^{M+1}\cos((M+1)(\theta-s)) + \frac{1}{2} - \frac{1}{2}\frac{r}{a}^2}{(\frac{r}{a})^2 - 2\frac{r}{a}\cos(\theta-s)+1}. \quad (12)$$

4 Results

In this section we demonstrate the effectiveness of the approximations by numerical experiments. In all cases, the number of evaluation points around each ring is $K = 12$.

Figure 2 shows the (absolute) relative error (defined as the absolute value of the ratio of error over true potential) as a function of radius for the outer ring approximation. The true values are calculated using the first part of equation 2. We note that the expansion appears accurate for all $r > b$ (and, indeed, may well be sufficiently accurate between the two rings).

Figure 3 shows the relative error as a function of radius for the inner ring approximation. Again, we note that the expansion appears accurate for all $r < a$ (and, indeed, may well be sufficiently accurate between the two rings).

Finally, using the same sources as in table 1 we set $M = \infty$ in equation 9 and we note that the resulting approximation shown in figure 4 is not as accurate close to the rings. This confirms the same behaviour as observed by Anderson [And92] for his combination of log potentials.

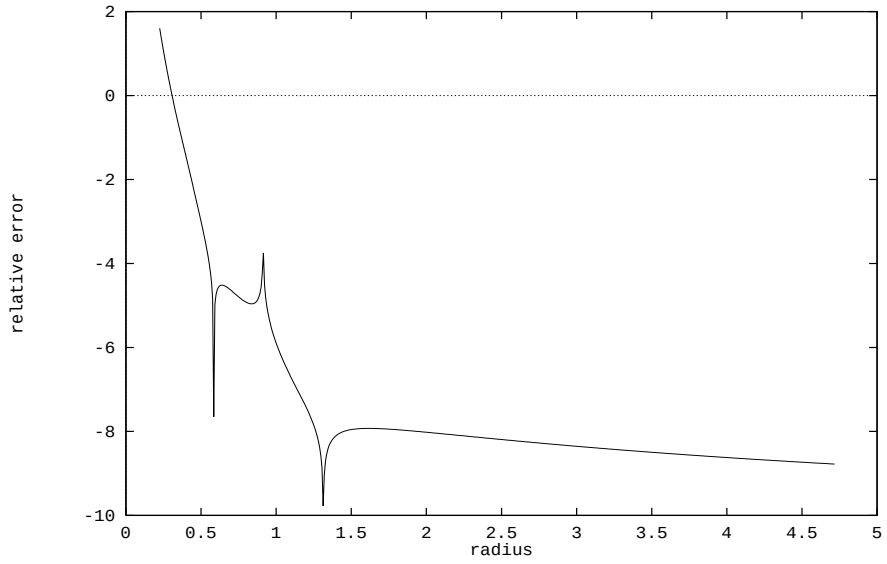

Figure 2: Outer Ring Approximation - Relative Error
The relative error in the approximation to $\Phi(r,\theta)$ versus radius taken along a line at orientation $\theta = 0$. The inner ring has radius $a = 0.75$ and the outer ring has radius $b = 1.25$. The 10 "sources", see table 1, were placed in a square of side length 1.0 centred on $(0,0)$. Note: relative error is shown on a logscale (base 10.)

Magnitude	Coordinates	
0.776471	-0.00588235	0.00588235
0.419608	-0.205882	0.484314
0.886275	0.484314	-0.170588
0.964706	0.241176	0.37451
0.486275	-0.390196	0.382353
0.529412	-0.496078	0.24902
0.192157	0.370588	-0.162745
0.447059	-0.441176	-0.221569
0.403922	-0.1	0.0294118
0.34902	0.166667	0.0333333

Table 1: 10 randomly chosen "sources" for the outer ring approximation.

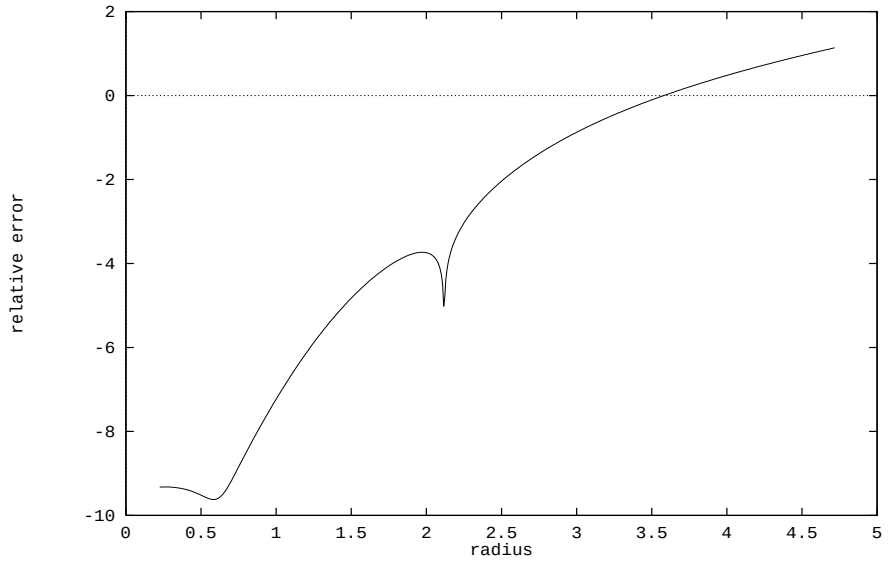

Figure 3: Inner Ring Approximation - Relative Error
The relative error in the approximation versus radius taken along a line at orientation $\theta = 0$. The inner ring has radius $a = 0.75$ and the outer ring has radius $b = 1.25$. The 10 "sources", see table 2, were placed in a square of side length 1.0 centred on $(2b, 0)$. Note: relative error is shown on a logscale (base 10.)

Magnitude	Coordinates	
0.776471	2.49412	0.00588235
0.419608	2.29412	0.484314
0.886275	2.98431	-0.170588
0.964706	2.74118	0.37451
0.486275	2.1098	0.382353
0.529412	2.00392	0.24902
0.192157	2.87059	-0.162745
0.447059	2.05882	-0.221569
0.403922	2.4	0.0294118
0.34902	2.66667	0.0333333

Table 2: 10 randomly chosen "sources" for the inner ring approximation.

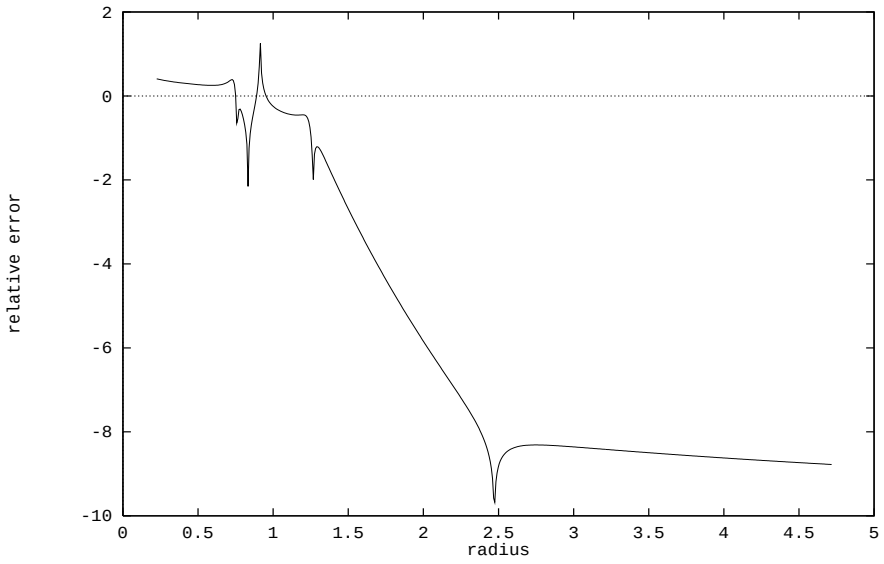

Figure 4: Outer Ring Approximation $M = \infty$ - Relative Error
The relative error in the approximation to $\Phi(r, \theta)$ versus radius taken along a line at orientation $\theta = 0$. The inner ring has radius $a = 0.75$ and the outer ring has radius $b = 1.25$. The 10 "sources", see table 1, were placed in a square of side length 1.0 centred on $(0.0, 0.0)$. Note: relative error is shown on a logscale (base 10.)

5 Conclusion

We have derived an approximation to the linear combination of the "potentials" derived from thin-plate spline formulations. These approximations are in the spirit of those introduced by [And92] to approximate the combination of potentials Φ satisfying Laplace's equation on the punctured plane (more specifically $\Delta\Phi = \delta$.) Building upon the work of Beatson and Newsam [BN92], we have derived and alternative approximation technique for kernels that are biharmonic on the punctured plane ($\Delta^2\Phi = \delta$.)

Like Beatson and Newsam, we feel that such approximations can lead to feasible approaches to spline formulations that involve several hundred or thousand data points. We also recognise the potential application areas in computer graphics and image processing (particle systems, image warping, and spline models of surfaces). The application areas we have immediately in mind are the spline formulations in visual reconstruction, particularly vector spline models of motion estimation [Sut92]. Indeed, the very nature of such problems is that one often obtains naturally clustered data points which leads to clusters of spline kernels.

However, in order to demonstrate fully the feasibility of such approaches we are currently working on a full system that incorporates hierarchical or multigrid like control and data structures (e.g., as outlined but not implemented in [And92] [BN92]). Clearly, there is also a need for better characterization of the error (preferably analytically derived bounds but also an empirical characterization of the size and dependence on various parameters such as the ring sizes a and b, the truncation point M, the number of integration points K, and the relative spread and position of the "sources" with respect to the rings.) We have already observed, as one would expect, a degradation in the approximation when the rings become less separated, and when the rings are too close to the sources. We have also confirmed that we get the same degradation as that that Anderson attributes to "aliasing" (when the truncation point

is determined by an M too large for the number of evaluation points.)

A Summation of Geometric Series

Define $\mathcal{Z} = \frac{a}{r}e^{\theta - s}$. Then, for arbitary limits L and M:

$$\begin{aligned} S &= \sum_{k=L}^{M} \mathcal{Z}^k && (13)\\ \mathcal{Z}S &= S + \mathcal{Z}^{M+1} - \mathcal{Z}^L && (14)\\ (\mathcal{Z}-1)S &= \mathcal{Z}^{M+1} - \mathcal{Z}^L && (15)\\ S &= \frac{\mathcal{Z}^{M+1} - \mathcal{Z}^L}{\mathcal{Z}-1} && (16)\\ &= \frac{\mathcal{Z}^{M+1} - \mathcal{Z}^L}{\mathcal{Z}-1}\frac{\overline{\mathcal{Z}}-1}{\overline{\mathcal{Z}}-1} \\ &= \frac{(\mathcal{Z}^M - \mathcal{Z}^{L-1})(|\mathcal{Z}|^2 - \mathcal{Z})}{|\mathcal{Z}|^2 + 1 - 2\mathcal{R}\{\mathcal{Z}\}} \end{aligned}$$

$$\mathcal{R}\{S\} = \frac{|\mathcal{Z}|^2\mathcal{R}\{\mathcal{Z}^M - \mathcal{Z}^{L-1}\} - \mathcal{R}\{\mathcal{Z}^{M+1} - \mathcal{Z}^L\}}{|\mathcal{Z}|^2 - 2\mathcal{R}\{\mathcal{Z}\} + 1} \quad (17)$$

B Inner Ring Approximation

We know [BN92] that, for a collection of points outside of a ring of some given radius, we can approximate the thin-plate potential within the disk by:

$$\Phi(z) = \mathcal{R}\left\{\sum_{l=0}^{\infty}(g_l\overline{z} + h_l)z^l\right\}. \quad (18)$$

Not surprisingly, the coefficients producing the singularities in equation 1 are zero as we have no singularities within the disk. Again, the values of the particular coefficients do not concern us as we produce an approximation by integrating the function over concentric circles.

In polar form:

$$\Phi(r,\theta) = \mathcal{R}\left\{\sum_{l=0}^{\infty}(g_{l+1}r^2 + h_l)r^l e^{il\theta} + g_0 r e^{-i\theta}\right\}. \quad (19)$$

Without loss of generality, we can define an new coefficient $h_1' = h_1 + g_0$ and set $g_0 = 0$ in the above expression (since the real parts of the terms involving h_1 and g_0 are equal to some constant times $r\cos\theta$.)

So we can see that for $l \geq 1$ (and using the new h_1):

$$\begin{aligned} \int_0^{\pi} \Phi(a,s)e^{-ils}\,ds &= \pi(g_{l+1}a^2 + h_l)a^l, && (20a)\\ \int_0^{\pi} \Phi(b,s)e^{-ils}\,ds &= \pi(g_{l+1}b^2 + h_l)b^l, && (20b) \end{aligned}$$

or for $l \geq 1$

$$g_{l+1} = \frac{1}{\pi}\frac{1}{a^2-b^2}\left(a^{-l}\int_0^{2\pi}\Phi(a,s)e^{-ils}\,ds\; -b^{-l}\int_0^{\pi}\Phi(b,s)e^{-ils}\,ds\right), \tag{21a}$$

$$h_l = \frac{1}{\pi}\frac{1}{a^2-b^2}\left(-b^2a^{-l}\int_0^{2\pi}\Phi(a,s)e^{-ils}\,ds\; +a^2b^{-l}\int_0^{\pi}\Phi(b,s)e^{-ils}\,ds\right). \tag{21b}$$

For the special cases g_1 and h_0 we obtain:

$$g_1 = \frac{1}{2\pi}\frac{1}{a^2-b^2}\left(\int_0^{2\pi}\Phi(a,s)\,ds\; -\int_0^{2\pi}\Phi(b,s)\,ds\right), \tag{22a}$$

$$h_0 = \frac{1}{2\pi}\frac{1}{a^2-b^2}\left(-b^2\int_0^{2\pi}\Phi(a,s)\,ds\; +a^2\int_0^{2\pi}\Phi(b,s)\,ds\right). \tag{22b}$$

On substituting into 19 (and truncating the series at $l = M$) gives:

$$\begin{aligned}\Phi(r,\theta) = \frac{1}{\pi}\frac{1}{a^2-b^2}\mathcal{R}\Bigg\{&\int_0^{2\pi}\\ &(r^2-b^2)\Phi(a,s)\left(\sum_{l=1}^{M}(\frac{r}{a})^l e^{il(\theta-s)}\right)+(a^2-r^2)\Phi(b,s)\left(\sum_{l=1}^{M}(\frac{r}{b})^l e^{il(\theta-s)}\right)\,ds\\ &+\frac{1}{2}\left(\int_0^{2\pi}(r^2-b^2)\Phi(a,s)\,ds+(a^2-r^2)\int_0^{2\pi}\Phi(b,s)\,ds\right)\Bigg\}.\end{aligned} \tag{23}$$

This can be re-written more compactly as:

$$\begin{aligned}\Phi(r,\theta) = \frac{1}{\pi}\frac{1}{a^2-b^2}\mathcal{R}\Bigg\{&\int_0^{2\pi}(r^2-b^2)\Phi(a,s)\left(\sum_{l=0}^{M}(\frac{r}{a})^l e^{il(\theta-s)}-\frac{1}{2}\right)\\ &+(a^2-r^2)\Phi(b,s)\left(\sum_{l=0}^{M}(\frac{r}{b})^l e^{il(\theta-s)}-\frac{1}{2}\right)\,ds\Bigg\}.\end{aligned} \tag{24}$$

We now sum the geometric series:

$$S = \sum_{l=0}^{M}(\frac{r}{a})^l e^{il(\theta-s)} \tag{25}$$

$$= \frac{(\frac{r}{a})^{M+2}e^{iM(\theta-s)}-(\frac{r}{a})^{M+1}e^{i(M+1)(\theta-s)}+1-\frac{r}{a}e^{-i(\theta-s)}}{(\frac{r}{a})^2-\frac{r}{a}e^{i(\theta-s)}-\frac{r}{a}e^{-i(\theta-s)}+1}. \tag{26}$$

Taking the real part:

$$\mathcal{R}\{S\} = \frac{(\frac{r}{a})^{M+2}\cos(M(\theta-s))-(\frac{r}{a})^{M+1}\cos((M+1)(\theta-s))+1-\frac{r}{a}\cos(\theta-s)}{(\frac{r}{a})^2-2\frac{r}{a}\cos(\theta-s)+1}. \tag{27}$$

Finally, we define $\mathcal{K}'(r,a,\theta,s,M) = \mathcal{R}\{S\}-\frac{1}{2}$:

$$\mathcal{K}'(r,a,\theta,s,M) = \frac{(\frac{r}{a})^{M+2}\cos(M(\theta-s))-(\frac{r}{a})^{M+1}\cos((M+1)(\theta-s))+\frac{1}{2}-\frac{1}{2}\frac{r}{a}^2}{(\frac{r}{a})^2-2\frac{r}{a}\cos(\theta-s)+1}. \tag{28}$$

C Acknowledgements

This is a correction of an earlier version. I thank G. K. Cambrell for numerous corrections to the earlier version. I also appreciate his suggested improvements and helpful criticisms.

References

[And92] C. R. Anderson. An implementation of the fast multipole method without multipoles. *Sci. J. Sci. Stat. Comput.*, 13(4):923–947, July 1992.

[BN92] R. K. Beatson and G. N. Newsam. Fast evaluation of radial basis functions: 1. *Comp. Math. Applic.*, to appear Oct/Nov. 1992.

[BZ87] A. Blake and A Zisserman. *Visual Reconstruction.* MIT Press, Cambridge MA, 1987.

[CGR88] J. Carrier, L. Greengard, and V. Rokhlin. A fast adaptive multipole algorithm for particle simulations. *SIAM J. Sci. Stat. Comput.*, 9(4):669–686, July 1988.

[LR70] N. Levinson and R. M. Redheffer. *Complex Variables.* Holden-Day, San Francisco, 1970.

[SNWC77] L. Sario, M. Nakai, C. Wang, and L. O. Chung. *Classification Theory of Riemannian Manifolds: Harmonic, quasiharmonic and biharmonic functions*, volume 605. Springer-Verlag, Berlin, 1977.

[Sut92] D. Suter. Efficient recovery of "time to crash" and rotation from optic flow. In *ICARCV-92 2nd International Conference on Automation, Robotics and Computer Vision*, volume 1, pages CV11.4.1–CV11.4.5, Singapore, September 1992. Institution of Engineers, Singapore.

[Ter82] D. Terzopoulos. Multi-level reconstruction of visual surfaces: Variational principles and finite element representations. Ai memo 671, MIT, April 1982.

[Wah90] G. Wahba. *Spline Models for Observational Data.* SIAM, Philadelphia, PA, 1990.